Determination of Vessel Heading using Magnetic Wake Imaging

Mohammad Amir Fallah[1*], Mehdi Monemi[2]

[1*]*Assistant Professor, Department of Engineering, Payame Noor University (PNU), Tehran, Iran; mfallah@shirazu.ac.ir*
[2] *Assistant Professor, Department of Electrical Engineering, Salman Farsi University of Kazerun, Kazerun, Iran; monemimahdi@gmail.com*

ARTICLE INFO	ABSTRACT

The small microwave skin depth of sea water as well as the small penetration depth of laser signal in water impose limitations on the application of SAR and Lidar in sea surveillance systems. On the other hand, vessels travelling at sea bring about hydrodynamic anomalies in the sea water called as wake. These hydrodynamic disturbances can be detected by using some techniques such as airborne radio imaging and Extremely Low Frequency (ELF) electromagnetic signal processing. In practice, the motion of conductive sea water anomalies in the natural earth's magnetic field induces ELF magnetic wakes which can be measured via accurate magnetic sensors and detected through signal processing schemes. The physical properties of the hydrodynamic wake as well as those relating to the corresponding magnetic wake are directly related to the vessel parameters such as hull shape, speed and heading. In this work, we firstly derive and formulate the mathematical expressions relating to the aforementioned hydrodynamic and magnetic wakes. By employing derived expressions, a novel detection scheme is proposed based on constructing the 2-dimentional image of the vessel's magnetic wake through the magnetic signals captured from an array of magnetic sensors, and finally, the relation between the spectral image of the magnetic wake and the vessel heading is studied. We will show that our proposed scheme can detect the existence of a remote vessel as well as its heading from the constructed image with high accuracy, and moreover, it does not have common limitations of existing single-sensor based heading detection schemes.

1. Introduction

The hydrodynamic wave at the sea surface created by the movement of a vessel is visible for airborne radars, Synthetic Aperture Radars (SAR) and lidars [1-7]. Once a high-quality signal is measured through a sensor, the implementation of signal processing techniques is required in order to accurately distinguish the signal from remote vessel out of environmental noise and disturbances [8-10]. The employment of radar and lidar systems, even with efficient signal processing schemes, is not effective for many situations in the sea surveillance systems. The main reason for this inefficiency is the large power loss of high frequency electromagnetic waves in the sea water resulting in low effective detection range.

Traveling vessels bring about hydrodynamic anomalies called as wakes [10-14] in electrically conductive seawater across the ambient earth magnetic field, leading to the induction of magnetic wakes [15-19].

Efficient implementation of remote sensing schemes for vessels through electromagnetic signal measurement requires highly accurate magnetic sensors. Moreover, due to the large dimensions of hydro-physical changes, hydrodynamic harmonics in the seawater are considered as low frequency ones. Therefore, accurate magnetic sensors with accuracy of less than 1 pico-Tesla (pT) and low frequency measuring capability is essential for the implementation of efficient remote sensing techniques [20, 21]. The low frequency induced hydromagnetic wakes can be measured and detected through magnetic sensors positioned at the sea surface or under the sea surface. Although dimensions of marine vehicles are limited, the generated wakes may extend tens of kilometers and remain for several hours under certain conditions [10-13].

The Induced magnetic wake of a ship in an infinite depth sea was studied by Madurasinghe [17-19]. Zou and Nehorai [22-24] proposed a single-sensor detection scheme by using an airborne magnetometer flying above an infinite depth sea. The proposed detection method suffers from several drawbacks including the

detection limitation of the angle between the vessel heading and magnetic sensor trajectory (which should be lower than 19.47^0 in order to be detectable [22]), as well as the impossibility of distinguishing the positive heading angles from negative ones. In addition, in the airborne method, it is possible to track the aircraft and destroy it, but in the proposed single-sensor method, this problem is solved.

When a marine surveillance system observes the footprint of a vessel by capturing the magnetic wake samples through magnetic sensors, the next step is to process the received signal in order to detect the existence of a remote floating vessel or submarine as well as distinguishing the physical parameters of the traveling body such as heading, velocity, size, and hull shape. This post processing step is done by formulating the dependency of the magnetic wake to the vessel parameters. In order to overcome the drawbacks of the single-sensor heading detection scheme as stated above, in this work, we firstly derive and formulate the mathematical expressions relating to the hydrodynamic and magnetic wakes, and then a magnetic sensor array structure is proposed in order to measure the magnetic wake of the remote vessel. By employing the derived expressions, and based on different time delay of the magnetic wake signals measured through each element of the sensor array, the magnetic image of the vessel wake is constructed, and finally, the relation between the captured image of the magnetic wake and the vessel heading is studied. We will show that the vessel heading can be obtained from the spectral image of the magnetic wake in the presence of ambient Gaussian noise.

2. Mathematical Formulation

Consider the free space in the Cartesian coordinate system wherein the fluid surface corresponds to the plane $z = 0$ which is perfectly flat. We consider two electromagnetic media; the air and the fluid corresponding to the space regions $z > 0$ and $z < 0$ respectively. Electric conductivity, susceptibility and magnetic permeability of these layers are denoted by (σ_a, ε_a, μ_a) and (σ_w, ε_w, μ_w) respectively. Both media are immersed in natural earth magnetic field $\boldsymbol{B}_E$. By default, we assume that the vessel travels in the x-axis direction, and the z-axis is perpendicular to the fluid surface. The more general case wherein the vessel heading is an arbitrary direction (other than the x-axis) is later studied in Section 5.

Assuming the sea water is an irrotational fluid, which is acceptable at far distances away from the vessel, the induced magnetic wake at point (x, y, z) instigated by a moving vessel can be written as [17-19]:

$$\boldsymbol{H}(x, y, z)$$
$$= \Re e \int_{-\pi/2}^{\pi/2} \boldsymbol{h}(\theta, z) A_\theta \, e^{-i(k_0 x \cos\theta + k_0 y \sin\theta)} \, d\theta \qquad (1)$$

Wherein

$$A_\theta = \frac{2UVk_0^2}{\pi L} \, \text{Koch}(\theta) \qquad (2a)$$

$$k_0 = \left(\frac{g}{U^2}\right) sec^2\theta$$
$$\omega_0 = k_0 \cos\theta \qquad (2b)$$

$$\text{Koch}(\theta) =$$
$$\iint_s I_\kappa(x', y', z') e^{-ik_0 x' \cos\theta} \cosh k_0(z' + d) dx' dz' \qquad (2c)$$

and

$$i = \sqrt{-1} \, , \qquad g = 9.8 \, ^m/_{s^2}$$

wherein $\text{Koch}(\theta)$ is the Kochin function [12], $s(x', y', z')$ is the wetted part of the submerged portion of the vessel hull and $I_\kappa(x', y', z')$ represents the intensity of pressure distributed on the hull. The unknown term $\boldsymbol{h}(\theta, z)$ can be calculated by applying continuity conditions of normal component of $\boldsymbol{B}$ and tangential component of $\boldsymbol{H}$ in the surface between the air and the water which can be obtained as :

$$\boldsymbol{h}(\theta, z) = \boldsymbol{h}^a(\theta, z) \qquad (3)$$
$$= \boldsymbol{P} e^{\delta z} \frac{\boldsymbol{a}(\theta)}{(k_0^2 - \delta^2)} e^{k_0 z} \qquad \text{for } z < 0$$

$$\boldsymbol{h}(\theta, z) = \boldsymbol{h}^w(\theta, z)$$
$$= \left[\boldsymbol{P} \frac{\boldsymbol{a}(\theta)}{(k_0^2 - \delta^2)}\right] e^{\beta z} \qquad \text{for } z > 0$$

in which

$$\boldsymbol{P} = \qquad\qquad\qquad\qquad\qquad (4)$$
$$\frac{(\beta + k_0)}{(\beta + \delta)} \frac{\boldsymbol{a}(\theta).\boldsymbol{k}}{(k_0^2 - \delta^2)} \left(\frac{\delta \cos\theta}{ik_0}, \frac{\delta \sin\theta}{ik_0}, 1\right)$$

$$\boldsymbol{a}(\theta) =$$
$$\sigma_0 k_0 \{(\boldsymbol{B}_E.\boldsymbol{k}) - i(\boldsymbol{B}_E.\boldsymbol{i} \cos\theta + \boldsymbol{B}_E.\boldsymbol{j} \sin\theta)\}.$$
$$(\boldsymbol{i} \cos\theta + \boldsymbol{j} \sin\theta - \boldsymbol{k})$$

$$\beta^2 = k_0^2 - \varepsilon_0 \mu \omega_0^2$$
$$\delta^2 = k_0^2 - \varepsilon_0 \mu \omega_0^2 - i\sigma_0 \mu \omega_0$$
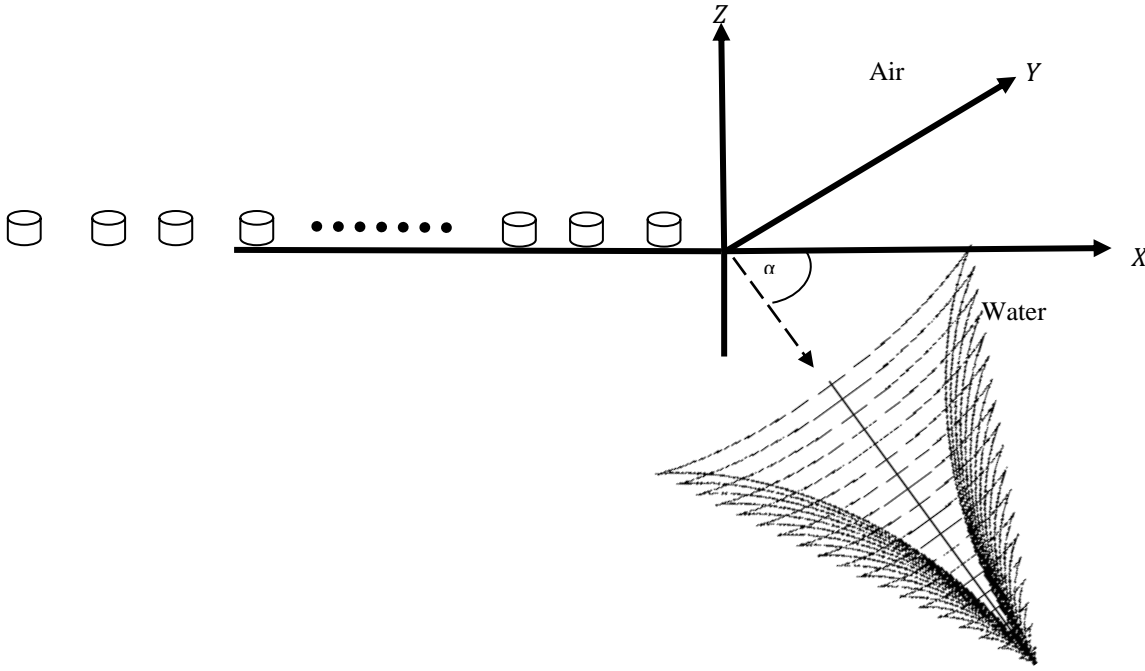
Figure 1. Configuration of the sensor array in the x-axis. The vessel is assumed to travel at the direction corresponding to the dashed line whose angle is α relative to the x-axis.

3. Spectral Analysis

In what follows we study the frequency spectrum of the magnetic wake as a means that sheds light on how the vessel heading can be distinguish from the spectral image of its magnetic wake. The spectrum of the magnetic anomaly is obtained by taking the spatial Fourier transform of magnetic wake in the points located on the plane parallel to the xy plane and located at the altitude $z = z_0$ which is expressed as follows:

$$
\begin{aligned}
\widehat{H}(X,Y) &= \int_{-\infty}^{\infty} \int_{-\infty}^{\infty} H^a(x,y,z_0)\, e^{-i2\pi(Xx+Yy)}\, dx\, dy \\
&= \frac{h^a(\theta,z_0)A_\theta}{\left|\frac{\partial}{\partial\theta}(X-X_0)\right|\left|\frac{\partial}{\partial\theta}(Y-Y_0)\right|}\, \delta(\theta_x - \theta_y)
\end{aligned}
\tag{5}
$$

where

$$
X_0 = \frac{k_0\cos\theta}{2\pi} \quad , \quad Y_0 = \frac{k_0\sin\theta}{2\pi}
\tag{6}
$$

and (θ_x, θ_y) are obtained by solving the following equations:

$$
X - X_0 = 0 \quad , \quad Y - Y_0 = 0
\tag{7}
$$

The solution to equation (5) represents a locus on the $z = z_0$ plane describing the vessel's magnetic wake spectrum. Referring to (6) and (7), it is inferred that the spectrum consists of a number of impulses with intensity $\dfrac{h^a(\theta,z_0)A_\theta}{\left|\frac{\partial}{\partial\theta}(X-X_0)\right|\left|\frac{\partial}{\partial\theta}(Y-Y_0)\right|}$ at points corresponding to $\theta = \theta_x = \theta_y$.

4. Sensor Array Configuration

Assume that M magnetic sensors are positioned along the x-axis as shown in Figure 1. The vessel is assumed to travel at the direction corresponding to the dashed line whose angle is α relative to the x-axis. This configuration has a time-spatial nature, in the sense that all magnetic sensors are fixed and simultaneously receive magnetic signal samples with sampling period $T_s = {1}/{f_s}$ in time domain, and at M location points in the spatial domain. As the time passes, the xy-plane magnetic image is constructed through processing the received signals at the M location points and N time-steps. It is obvious that increasing the number of receiving sensors as well as the acquisition time leads to higher resolution of the magnetic image resulting in better detection probability. The image resolution in the spatial domain depends on the number of magnetic sensors positioned at the x axis, and on the other hand, the image clarity in time domain increases as time passes. Finally, the array can construct the magnetic image of the vessel wake and determine the vessel heading as described in the following section.

5. Determination of vessel heading

The shape of the magnetic wake is directly related to the vessel traveling direction and any change in the vessel heading leads to variations in the image of the wake; this is an important factor to be considered in the

estimation of the vessel heading. To show this key relation, assume that the angle between the vessel heading and the sensors array axis is denoted by α. It is evident that the received magnetic image in this case (denoted by $\boldsymbol{H}'$) is the same as that presented for $\alpha = 0$ (denoted by $\boldsymbol{H}$ as expressed in previous sections) except that it is rotated by α degrees in the counterclockwise direction. In what follows we prove that the spatial spectral Fourier transform for $\boldsymbol{H}'$ is also a rotation of that for $\boldsymbol{H}$ by α derees. Let define

$$(x', y') = \mathcal{R}\{(x, y), \alpha\} \tag{8a}$$
$$\boldsymbol{H}'(x', y') = \mathcal{R}\{\boldsymbol{H}(x, y), \alpha\} \tag{8b}$$

where the operator $\mathcal{R}\{\boldsymbol{f}(x, y), \alpha\}$ rotates $\boldsymbol{f}(x, y)$ by α degrees in the counterclockwise direction. According to (5), the spectrum of the received magnetic signal is expressed as:

$$\mathcal{F}\{\boldsymbol{H}'(x', y')\}(X', Y') =$$
$$\int_{-\infty}^{\infty} \int_{-\infty}^{\infty} \boldsymbol{H}'(x', y', z_0) e^{-i2\pi(X'x' + Y'y')} dx' dy' \tag{9}$$

where $(X', Y') = \mathcal{R}\{(X, Y), \alpha\}$. Now, from (8b) we can write:

$$|\mathcal{F}\{H'(x', y')\}(X', Y')|$$
$$= \left| \int_{-\infty}^{\infty} \int_{-\infty}^{\infty} H'(x', y', z_0) e^{-i2\pi(X'x' + Y'y')} dx' dy' \right|$$
$$= $$
$$\left| \int_{-\infty}^{\infty} \int_{-\infty}^{\infty} H(x' \cos\alpha - y' \sin\alpha, x' \sin\alpha \right.$$
$$\left. + y' \cos\alpha, z_0) e^{-i2\pi(X'x' + Y'y')} dx' dy' \right| \tag{10}$$

On the other hand

$$|dxdy| = |h_1 h_2 \, dx' dy'| = 1 \tag{11}$$
where,

$$h_1^2 = \left(\frac{\partial x'}{\partial x}\right)^2 + \left(\frac{\partial y'}{\partial x}\right)^2 = 1$$
$$h_2^2 = \left(\frac{\partial x'}{\partial y}\right)^2 + \left(\frac{\partial y'}{\partial y}\right)^2 = 1 \tag{12}$$
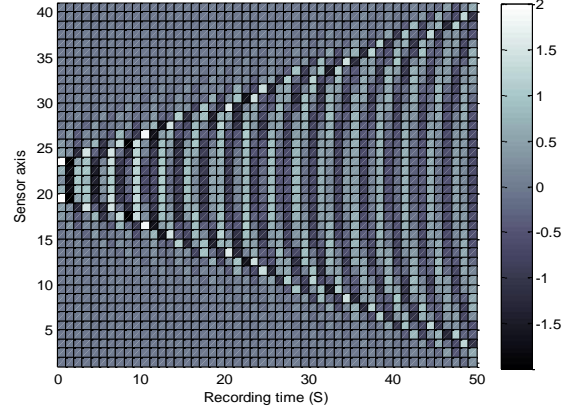
Hence we have:

and finally, we conclude that

Figure 2. Magnetic wake amplitude (nT) at vessel speed 10 m/s recorded by 40-element multi-sensor arrangement with $N = 50$ time-steps and $f_s = 0.5 \, Hz$ in a noiseless environment.

$$|\mathcal{F}\{\mathcal{R}(\boldsymbol{H}(x, y), \alpha)\}| = |\mathcal{R}(\mathcal{F}\{\boldsymbol{H}(x, y), \alpha\})| \tag{14}$$

In other words, adding the angle α between vessel trajectory and the sensors array axis leads to an image rotation equal to α in the spectral domain. Hence, determination of image rotation in spectral domain leads to the detection of vessel heading with respect to the array axis. Based on what stated, we propose the following heading detection scheme:

Algorithm 1: Determination of the vessel heading through constructing the spectral image of the magnetic wake

1- Let M and N be the total number of sensors and measuring time steps respectively.
2- For each $m \in \{1, 2, ..., M\}$ and $n \in \{1, 2, ..., N\}$, let $\widetilde{\boldsymbol{H}}[m, n]$ be the time domain magnetic signal measured by the m'th sensor at the n'th time step, where $\widetilde{\boldsymbol{H}}[m, n] = \boldsymbol{H}[m, n] + \sigma_{m,n}$ in which $\sigma_{m,n}$ is the corresponding Gaussian ambient noise.
3- Calculate the spatial Fast Fourier Transform (FFT) of $\widetilde{\boldsymbol{H}}_{MN}$ denoted by $\widetilde{\boldsymbol{H}}'_{MN}$ and depict the corresponding two-dimensional image of $\widetilde{\boldsymbol{H}}'_{MN}$.
4- Determine the direction of the wake by calculating the rotation angle α of $\widetilde{\boldsymbol{H}}'$ through simple image processing techniques.

$$\left| \int_{-\infty}^{\infty} \int_{-\infty}^{\infty} H(x' \cos\alpha - y' \sin\alpha, x' \sin\alpha + y' \cos\alpha, z_0) e^{-i2\pi(X'x' + Y'y')} dx' dy' \right| =$$
$$\left| \int_{-\infty}^{\infty} \int_{-\infty}^{\infty} H(x, y, z_0) . e^{-i2\pi(x(X' \cos\alpha - Y' \sin\alpha) + y(X' \sin\alpha + Y' \cos\alpha))} dx dy \right| =$$
$$|\mathcal{F}\{H(x, y, z_0)\}(X' \cos\alpha - Y' \sin\alpha, X' \sin\alpha + Y' \cos\alpha, z_0)| = |\mathcal{R}(\mathcal{F}\{H(x, y), \alpha\})|$$
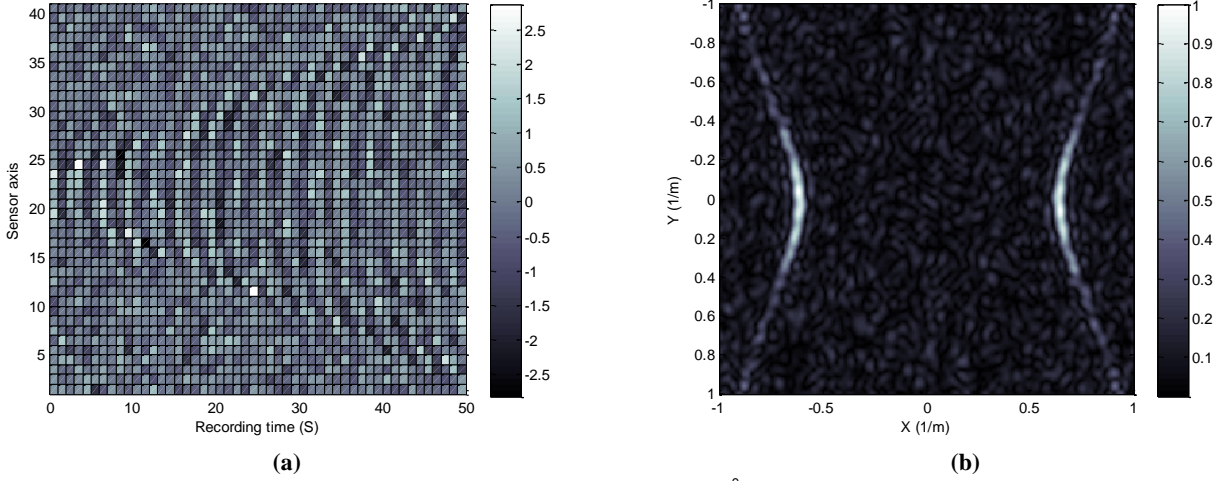
$$\tag{13}$$

(a)   **(b)**

Figure 3. (a) Magnetic wake amplitude (nT) at vessel speed 10 m/s, $\alpha = 0°$ and SNR=0 dB recorded by 40-element sensor array arrangement with $N = 50$ time-steps and $f_s = 0.5\ Hz$. (b) Normalized spectrum of the corresponding magnetic wake.

In the following section, we study through numerical results how the proposed scheme results in the determination of the vessel heading in different practical scenarios.

6. Numerical Results

In this section, we study the determination of vessel heading by exploring the magnetic wake instigated from a vessel traveling at different speeds and directions in the presence of background Gaussian noise. The dielectric susceptibility, electric conductivity and magnetic permeability in the air and water are assumed to be $(\varepsilon_a, \varepsilon_w) = (\varepsilon_0, 81\,\varepsilon_0)$, $(\sigma_a, \sigma_w) = (0,5)$ and $(\mu_a, \mu_w) = (\mu_0, \mu_0)$ respectively [25-28].

It is assumed that all sensor elements of the array are omnidirectional and uniformly arranged along the x-axis. The results are obtained by simulating the proposed scheme for a Wigley's hull ship with length

180 meters, draft 10 meters and beam 20 meters sailing at 10m/s. The magnetic wake induced by the hydrodynamic wake of the ship is observed by a 40-elements sensor array system with 20 meters spacing between adjacent sensor elements. The sampling rate is $f_s = 0.5$ Hz and the number of measuring time-steps is $N = 50$. Figure 2 is the time-domain magnetic wake image of $\widetilde{H}_{40\times50}$ captured through Algorithm 1 in a noiseless environment for $\alpha = 0°$. It is seen that the direction of the vessel movement is simply distinguished from the time-domain image and there is no need here to calculate the spectrum of $\widetilde{H}$.

In order to evaluate the performance of our proposed scheme and investigate the superiority of the proposed sensor array configuration to conventional single-sensor methods in vessel heading estimation, several cases are simulated in the following.

First, we consider that the vessel sails at speed 10m/s and $\alpha = 0°$ for the case when the signal to noise ratio
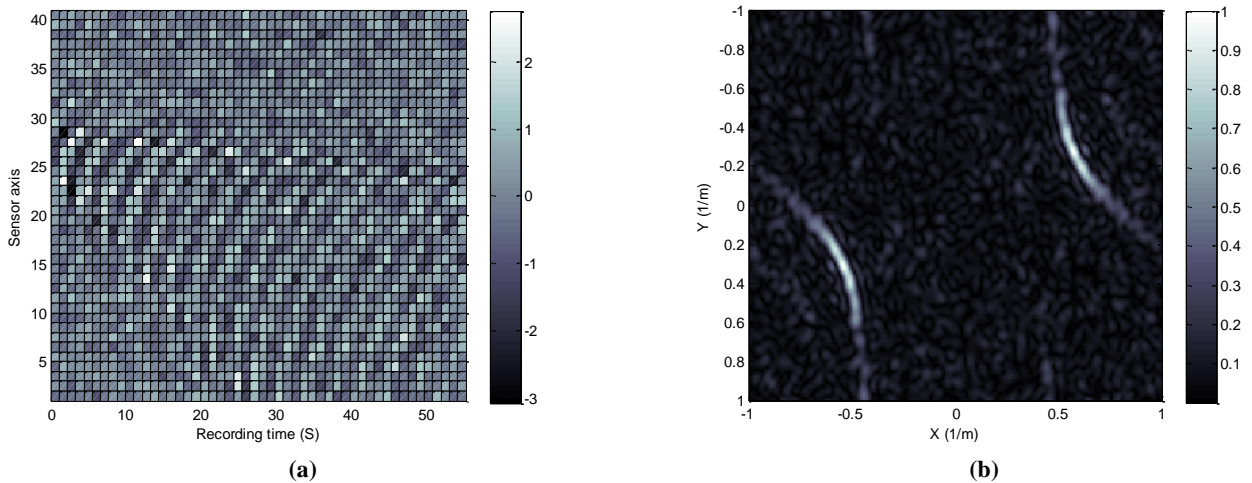

(a)   **(b)**

Figure 4. (a) Magnetic wake amplitude (nT) at vessel speed 10 m/s, $\alpha = 25°$ and SNR=0 dB recorded by 40-element array sensor arrangement with $N = 50$ and $f_s = 0.5\ Hz$ (b) Normalized spectrum of the corresponding magnetic wake.

Figure 5. (a) Magnetic wake amplitude (nT) at vessel speed 10 m/s, $\alpha = -35°$ and SNR=0 dB recorded by 40-element array sensor arrangement with $N = 50$ and $f_s = 0.5\ Hz$ (b) Normalized spectrum of the corresponding magnetic wake.
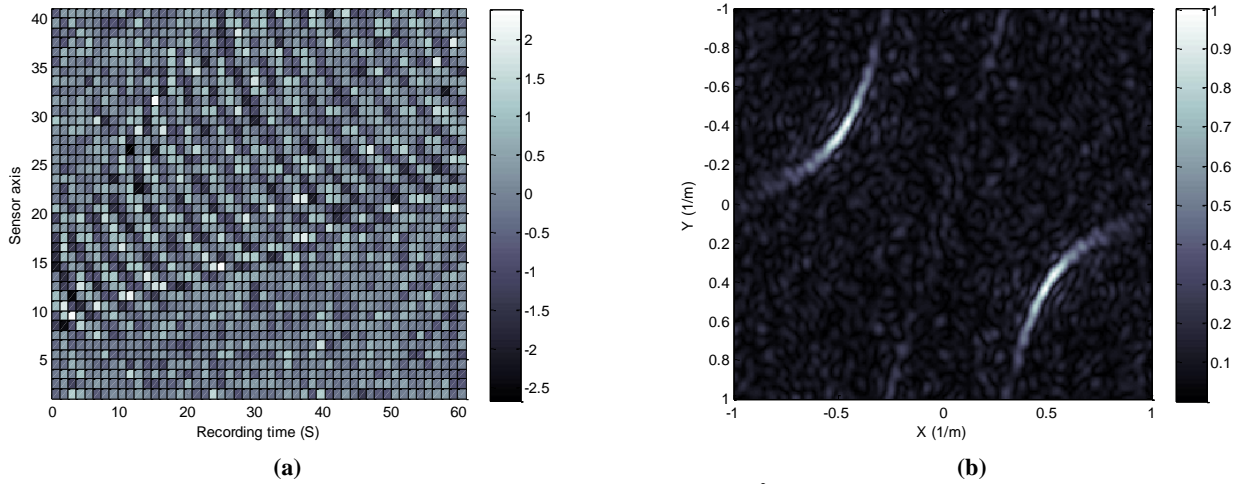
(SNR) is 0 dB. The obtained time-domain magnetic wake signal captured by the sensor array system is shown in Figure 3(a), and the corresponding magnetic wake spectrum calculated by using 512 points FFT is presented in Figure 3(b). Note that although the presence of the wake is not so clear in the time domain, in the spectral domain however, we can observe a clear indication of the presence of the vessel and distinguish the corresponding heading. This can be justified by the existence of delta functions in (5) and noting that the noise power spectrum is randomly distributed in the region of spectral plane.

Figure 4(a) and 4(b) display the magnetic wake and its spectrum for the same scenario as in Figure 3 except that $\alpha = 25°$ is considered here. The results show that that the limitation of conventional single sensor method in the vessel heading for $|\alpha| < 19.47°$ ([22]) does not exist here by using the proposed array sensor configuration. As seen in Figure 4(b), the spectral image of the magnetic wake is rotated counterclockwise around the image center by $\alpha = 25°$ as was pointed out in section 5. While the heading cannot be easily distinguished from the time-domain image in Figure 4(a), this is clearly detected in the spectral image in Figure 4(b).

Another advantage of the proposed detection scheme based on the spectral image construction through the sensor array configuration is to discriminate between positive and negative values of α which is impossible in the single sensor schemes [22]. Figure 5(a) and 5(b) show the magnetic time and spectral domain image of the magnetic wake for the same scenario as in Figure 4 wherein all parameters are the same as before except that heading direction corresponds to $\alpha = -35°$. Compared to the pervious case, the spectral image in this case rotates clockwise, and it is clearly seen that, negative values of the angle corresponding to the heading is easily detected as well.

7. Conclusion

In this paper we proposed the heading estimation of remote vessels by processing the magnetic wake of the vessel through an array of magnetometers. More specifically, we proposed a scheme to construct the magnetic image of the vessel wake and then obtained the corresponding spectral domain image. We verified through numerical results that our proposed scheme can estimate the heading of a remote vessel with relatively high accuracy in the presence of background Gaussian noise and moreover, the proposed method was shown to overcome the limitations of conventional single-sensor heading estimation techniques.

8. References

1- O. Karakuş and A. Achim, (2021), *On Solving SAR Imaging Inverse Problems Using Nonconvex Regularization With a Cauchy-Based Penalty*, IEEE Transactions on Geoscience and Remote Sensing, vol. 59, no. 7, p.5828-5840, doi: 10.1109/TGRS.2020.3011631.

2- O. Karakuş, I. Rizaev and A. Achim, (2020), *Ship Wake Detection in SAR Images via Sparse Regularization*, IEEE Transactions on Geoscience and Remote Sensing, vol. 58, no. 3, p.1665-1677, doi: 10.1109/TGRS.2019.2947360.

3- K. -m. Kang and D. -j. Kim, (2019), *Ship Velocity Estimation from Ship Wakes Detected Using Convolutional Neural Networks*, IEEE Journal of Selected Topics in Applied Earth Observations and Remote Sensing, vol. 12, no. 11, p. 4379-4388, doi: 10.1109/JSTARS.2019.2949006.

4- Grishin, M.Y., Lednev, V.N., Pershin, S.M. et al., (2021), *Lidar sensing of ship wakes*, Phys. Wave Phen. 25,p.225–230, https://doi.org/10.3103/S1541308X17030104.

5- Alexey F. Bunkin, Vladimir K. Klinkov, Vladislav A. Lukyanchenko, and Sergey M. Pershin, (2011), *Ship wake detection by Raman lidar*, Appl. Opt. 50, p.86-89.

6- G. Yang, J. Yu, C. Xiao and W. Sun, (2016), *Ship wake detection for SAR images with complex backgrounds based on morphological dictionary learning*, IEEE International Conference on Acoustics, Speech and Signal Processing (ICASSP), p. 1896-1900, doi: 10.1109/ICASSP.2016.7472006.

7- G. Zilman, A. Zapolski and M. Marom, (2014), *On detectability of a ship's Kelvin wake in simulated SAR images of rough sea surface* , IEEE Trans. Geosci. Remote Sens., vol. 53, no. 2, p.609-619.

8- Yingfei Liu, Jun Zhao, Yan Qin, (2021), *A novel technique for ship wake detection from optical images*, Remote Sensing of Environment, Volume 258.

9- Liu, Yingfei & Deng, Ruru. (2018). *Ship Wakes in Optical Images*. Journal of Atmospheric and Oceanic Technology. 35. 10.1175/JTECH-D-18-0021.1.

10- M. Gilman, A. Soloviev and H. Graber, (2011), *Study of the Far Wake of a Large Ship*, J. Atmos. Oceanic Technol., vol. 28, p.720–733.

11- J. N. Newman, (1977), *Marine hydrodynamics*, MIT Press, Cambridge, Massachusetts.

12- Kostyukov, A. A., (1968), *Theory of Ship Waves and Waves Resistance*, Effective Communications Inc., Iowa City. p.241-243.

13- Tuck, E. O., Collins, J. I., and W. H. Wells, (1971), *On Ship Wave Patterns and Their Spectra*, J Ship Res 15,p11–21.
doi: https://doi.org/10.5957/jsr.1971.15.1.11.

14- D. F. Gu and O. M. Phillips,(1988), *On narrow V-like ship wakes*, J. Fluid Mech., vol. 275, p.301–321.

15- Weaver, J. T., (1965), *Magnetic Variations Associated with Ocean Waves and Swell*, Journal of Geophysical Research, 70: p.1921–1929.

16- Sanford, T. B.,(1971),*Motionally Induced Electric and Magnetic Fields in the Sea*, Journal of Geophysical Research, 76: p.3476–3492.

17- D. Madurasinghe,(1994), *Induced* electromagnetic fields associated with large ship wakes,Wave Motion, 20, p.283–292.

18- D. Madurasinghe, E.O. Tuck,(1994), The induced electromagnetic field associated with submerged moving bodies in an unstratified conducting fluid, IEEE Journal of Ocean Engineering, 19 ,p.193–199.

19- D. Madurasinghe, GR. Haack, (1994), The induced electromagnetic field associated with wakes-signal processing aspects. Proceedings of IGRASS 94, Pasadena, CA, p.2335–2357.

20- Yijin Xie, Huiyao Yu, Yunbin Zhu, Xi Qin, Xing Rong, Chang-Kui Duan, Jiangfeng Du, (2021), A hybrid magnetometer towards femtotesla sensitivity under ambient conditions, Science Bulletin, Volume 66, Issue 2, P.127-132.

21- Deans, Cameron & Marmugi, Luca & Renzoni, Ferruccio. (2018), Sub-picotesla widely tunable atomic magnetometer operating at room-temperature in unshielded environments, Review of Scientific Instruments. 89. 083111. 10.1063/1.5026769.

22- N. Zou and A. Nehorai, (2000), *Detection of ship wakes using an airborne magnetic transducer*, IEEE Transactions on Geoscience and Remote Sensing, vol. 38, no. 1, p.532-539, doi: 10.1109/36.823948.

23- O. Yaakobi, G. Zilman, T. Miloh, (2011), *Detection of the electromagnetic field induced by the wake of a ship moving in a moderate sea state of finite depth*,J. Engrg. Math. 70,p.17–27.

24- XiangmingGuo, Dongliang Zhao, Zhongqing Cao,(2016), *Detection of the Magnetic Field Induced by the Wake of a Moving Submerged Body Using Simple Models,* American Journal of Electromagnetics and Applications. Vol. 4, No. 2, p.20-25. doi: 10.11648/j.ajea.20160402.12.

25-Robert, P., (1988). *Electrical and Magnetic Properties of Materials*, Artech House.

26- Schon, J.H., (1996), *Physical properties of rocks: fundamentals and principles of petrophysics Calculated from field data at Otis MMR*, Cape Cod, Massachusetts.

27- Mavko, G., (1998). *The rock physics handbook: tools for seismic analysis in porous media*.

28 - Carmichael, Robert S., (1989), *Practical handbook of physical properties of rocks and minerals*.